Cell Prof. 1998, **31**, 93–110

A dynamic model of proliferation and differentiation in the intestinal crypt based on a hypothetical intraepithelial growth factor

T. G. Gerike, U. Paulus,* C. S. Potten† and M. Loeffler

*Institut für Medizinische Informatik, Statistik und Epidemiologie, Leipzig; *Medizinische Klinik I, Abteilung Biometrie, LFI Ebene 5, Köln, Germany; and †CRC Department of Epithelial Cell Biology, Paterson Institute for Cancer Research, Christie Hospital & Holt Radium Institute, Manchester, UK*

(*Received* 29 *April* 1998; *accepted* 19 *May* 1998)

Abstract. A widely accepted model of the temporal and spatial organization of proliferation and differentiation in intestinal epithelia is based on a cellular pedigree with all cells descending from a few active stem cells and undergoing a sequence of transitory divisions until the non-proliferating maturing cell stages develop. Model simulations have shown that such a pedigree concept can explain a large variety of data. However, so far there is neither a direct experimental proof for the existence of an intrinsic age structure in the transitory proliferative cell stages nor for the distinction between stem and transitory cells. It is our objective to suggest an alternative model which is based on evidence for intercellular communications such as might be mediated through gap junctions. We consider the diffusion of a hypothetical intraepithelial growth factor in a chain of cells which are connected via gap junctions. Individual cells can divide if a critical growth factor concentration is exceeded. Simulation studies show that the model is consistent with many observed features of the small intestinal crypt in steady state and after perturbation.

The small intestinal tract is lined by a polarized monolayer epithelium which is folded into crypts and villi. The crypts in the small intestine of mice contain about 250 cells, of which 150 are rapidly proliferating with a cell cycle time of approximately 12 h in the lower two-thirds of the crypt (Al-Dewachi *et al.* 1975, 1979, Potten, Booth & Pritchard 1997a). Proliferation is restricted to the crypts. Cell differentiation and function takes place primarily in the upper parts of the crypts and on the villi.

Further evidence exists that the proliferative cells can be subdivided into self-regenerating stem cells which are located at the crypt-base and can maintain the tissue in the long run, and some proliferative cells that lack the stem cell property (Potten & Loeffler 1990, Potten *et al.* 1997a). These findings have prompted us and others to postulate a cellular pedigree concept in which a highly structured cellular development generates non-proliferating, maturing cells from a few active stem cells by undergoing a precisely determined sequence of transitory cell divisions. This concept assumes that decisions are made, either upon or after a stem cell division, as to whether a daughter cell remains a stem cell or whether it enters the first transitory cell stage. This concept operates on assumptions about conditions and

Correspondence: Professor M. Loeffler, Institut für Medizinische Informatik, Statistik und Epidemiologie, Liebigstraße 27, 04103 Leipzig, Germany.

programs that are self-sufficient in the cells and do not require communication between cells, except for stem cells which need to regulate their number (Loeffler & Potten 1997). This pedigree concept proved to be powerful in model-based simulations of a variety of experimental findings (Appleton *et al.* 1983, Meinzer & Sandblad 1986, Loeffler *et al.* 1986, Appleton 1990, Potten & Loeffler 1990, Paulus, Potten & Loeffler 1992, Paulus *et al.* 1993). Some of these models describe the temporal and spatial dynamics of the system on the basis of spatial cellular automata. They link cellular development, cell division and cell migration. These models consistently describe the spatial distribution of proliferating cells in the steady-state situation. The spatial arrangement of the cells after severe damage, as inflicted by high-dose irradiation, appears to be more complicated and is presently not well described by these models. However, modelling ignoring spatial information was undertaken by compartment models (Paulus *et al.* 1992) which suggest that the transitory cells need to respond more flexibly than permitted in the pedigree concept and some of them temporarily have to behave like stem cells. A more flexible view about stem cells is further supported by the observation that the number of clonogenic cells capable of giving rise to the epithelium may be larger than the number of stem cells active at any given point in time (Potten & Loeffler 1990, Hendry, Roberts & Potten 1992). In addition there are no biological markers available so far to identify an age structure within the transitory cell stages. Therefore there is some doubt on the validity of the pedigree concept and it was our objective to search for alternative models with less restrictive assumptions on the distinction between stem and transitory cells and with more flexibility to respond to demands.

In the last decade evidence has emerged of the importance of growth factors in the gut epithelium. Polypeptides like epidermal growth factor (EGF), transforming growth factor (TGFα), keratinocyte growth factor (KGF) and insulin-like growth factor (IGF) show stimulatory effects on cell proliferation (Goodlad *et al.* 1987, Boismenu & Havran 1994, Khan *et al.* 1997, Steeb, Trahair & Read 1992, Potten *et al.* 1995). TGF-β is a potential inhibitor of epithelial proliferation in the gut (Barnard, Warwick & Gold 1993, Potten, Booth & Haley 1997b).

Cyclooxygenase (COX), and the two isoforms of this enzyme (COX-1 and COX-2) in prostaglandin E2 synthesis play an important role in proliferation control and the use of nonsteroidal anti-inflammatory drugs (NSAIDs) acting as cyclooxygenase-inhibitors lowers the risk of hyperproliferative growth (Gustafson-Svard *et al.* 1996).

Furthermore, lymphocytes in the connecting tissue underlying the epithelium may produce cytokines that play an important role in the regulation. T helper cells 1 (Th1) characterized by the *in vitro* production of interferon-γ (IFN-γ) stimulate, Th2 cells (IL-4, IL-5 and IL-9) suppress cell proliferation in the intestinal epithelium (Artis *et al.* 1998).

The mode of action of many of these factors still needs to be determined. Some may act through signalling systems activating intracellular proliferation regulators. Such intracellular activators may then propagate through the epithelial layer via gap-junction channels. Using freeze-fracture techniques and ink-microinjection into murine small intestinal epithelium, Bjerknes, Cheng & Erlandsen (1985) described an 'intercellular continuum' mediated by gap-junctions that connect the cells. They showed that low molecular weight substances can easily diffuse from cell to cell and suggested that this may play an important part in regulating cellular behaviour. The existence of gap-junctions in murine intestinal epithelium is also confirmed by Kataoka *et al.* (1989). The loss of intercellular communication via gap-junctions is associated with gastric ulcer formation in humans (Ohkusa *et al.* 1993).

It is the objective of our study to investigate whether a simple model for crypt-proliferation regulated by an intraepithelial and diffusible growth factor can explain major features of

steady state and post radiation recovery. We refer to data on positional ^{3}HTdR labelling indices, mitotic indices and percent labelled mitoses obtained in steady state and after various doses of radiation.

MATERIALS AND METHODS

Basic assumptions of the model

Assumption 1: one-dimensional chain of cells

The epithelium is modelled by a one-dimensional chain of cells to obtain a qualitative analogy to the array of cells in a section of intestinal crypts along the vertical proliferation and migration axis (see Figure 1). The chain is thought to extend from the bottom of the crypt to the tip of the villus. All cells can be localized by their position relative to the basal cell. All cells are connected by gap-junctions forming an intercellular intraepithelial continuum.

Assumption 2: cell kinetic properties

All columnar cells, except Paneth cells, are assumed to be alike and to have an identical proliferation potential. They undergo a cell cycle with a sequence of G_1, S, G_2 and M-phases. We assume a G_1 restriction point that can only be passed if the growth factor concentration in the respective cell exceeds a certain threshold. The threshold is assumed to be constant in time. All cells are assumed to have the same threshold. The non-proliferative functional Paneth cells in positions 1 to 3 have no ability to proliferate and are not connected with gap-junctions. If a cell passes the G_1 restriction point it proceeds through S and G_2-phases and undergoes mitosis. The division is symmetric with identical daughter cells. The growth factor is divided in equal parts to the daughter cells. Two daughter cells are inserted into the cell chain instead of the mother cell, both connected with gap-junctions.

Assumption 3: cell removal at the villus tip

Cell loss occurs regularly as a random process with constant intensity at the top end of the cell chain analogous to the cell loss at the real villus tip. The cell removal rate is assumed to be one cell per hour, similar to the measured cell migration velocity (Kaur & Potten 1986).

Assumption 4: ^{3}HTdR labelling

To compare the model with experimental data following injection of ^{3}HTdR we assume that all cells in S-phase can be labelled and that during cell division the label is passed to the daughter cells. Dilution of the label is not considered, which is justified as we do not regard more than three cell divisions after labelling.

Assumption 5: radiation damage

Radiation damage of the cells is considered in a simplified manner. We assume that an 8 Gy whole-body radiation damages 60% and that 12 Gy damages 90% of all columnar cells. The cells become sterile in terms of reproduction and therefore cannot pick up ^{3}HTdR label. Damaged cells do not disappear but are moved by passive migration caused by the proliferation of the remaining intact cells. However, it is assumed that radiation does not affect the intraepithelial growth factor diffusion. Thus apoptotic cell death is not considered.

Assumption 6: growth factor

Proliferation is controlled by an intraepithelial growth factor (GF). The GF is assumed to be a small molecule that has the ability to pass through gap-junctions between adjacent cells according to gradient driven diffusion. We assume a source for the GF production at the bottom of the crypt (either in the Paneth cells or in the first columnar cell). The diffusion process has a much smaller time constant (order of several minutes) than typical cell cycle times (order of several hours). The source produces GF at a constant rate. The GF undergoes a decay with a specific time constant. The GF enables the cells to proceed within the cell cycle and to pass the G_1 restriction point in G_1-phase if present in large enough

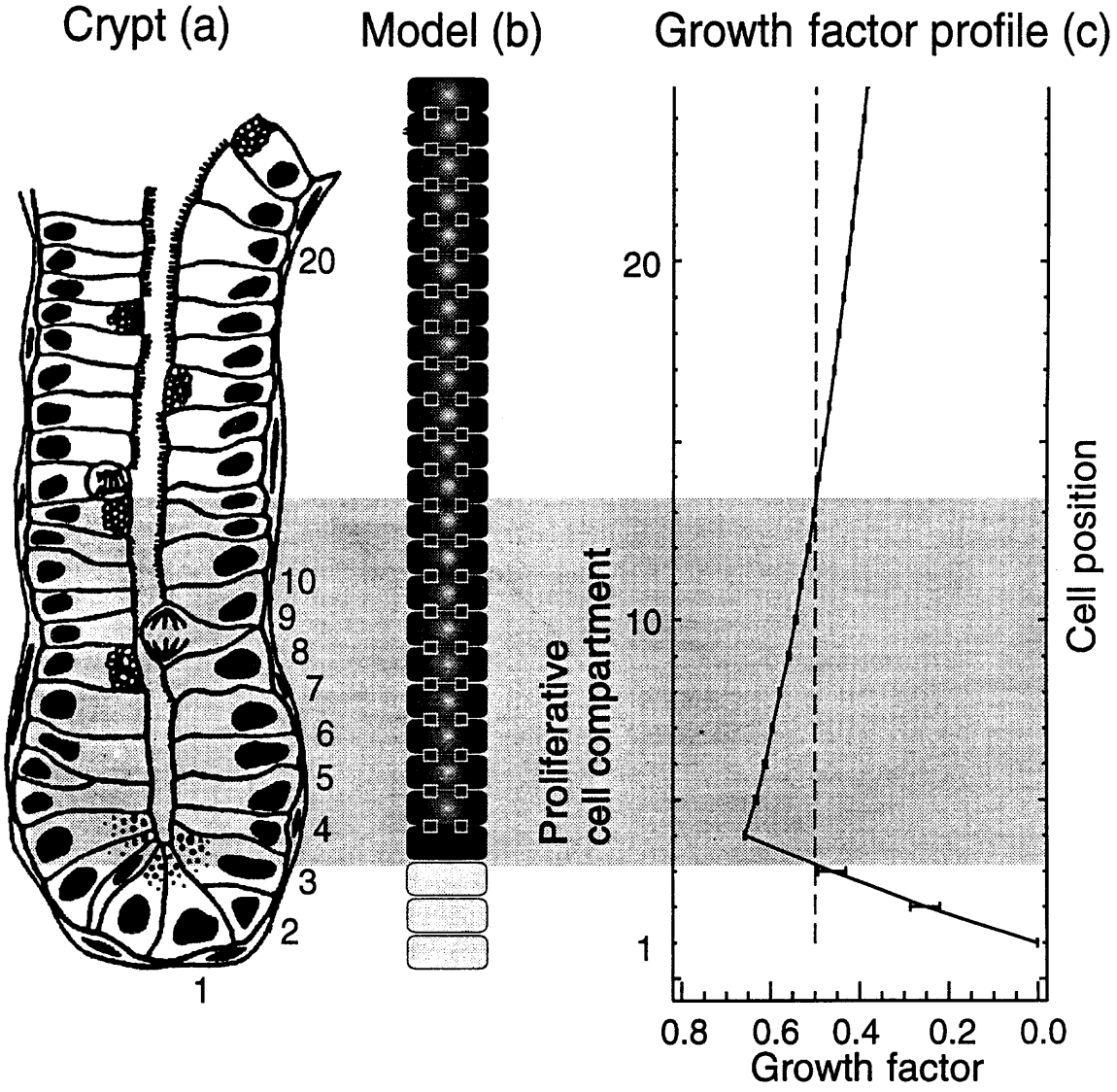

Figure 1. Diagram of the model approach. (a) Scheme of a longitudinal section of the murine small intestinal crypt with non-proliferative Paneth cells at the bottom of the crypt and the proliferative cell compartment in the highlighted area above. (b) One-dimensional model of the crypt with three non-proliferative Paneth cells at the bottom and a growth factor producing cell at position four (black). Potential proliferative cells at higher positions are connected by gap junctions (small black boxes). (c) Growth factor profile snapshot averaged over 100 model crypts. The decline in GF concentration at lower positions is caused by variable position of the GF producing cell. The number of Paneth cell. The decline in GF concentration with higher positions is caused by diffusion and decay. Cells with a GF concentration above a certain threshold (dashed line, highlighted zone) may proliferate.

concentrations. We assume that the GF diffuses through the gap-junctions according to Fick's law which had to be specified in a finite difference approximation:

$$\frac{\partial \varphi}{\partial t}=D\Delta\varphi \tag{1}$$

with substance concentration φ, diffusion constant D and Laplace operator $\Delta=\partial^2/\partial x^2$.

Applied to a cellular system, we assume a homogeneous distribution of the substance with the concentration $\bar{\varphi}$ in a cell with the volume V. Hence integration of equation (1) over the cell volume V gives

$$\frac{\partial}{\partial t}\int_V \varphi\, dV=V\frac{\partial}{\partial t}\bar{\varphi}=D\int_V \Delta\varphi\, dV$$

According to the Gaussian theorem one can convert a volume integral into an integral over the associated surface:

$$V\frac{\partial}{\partial t}\bar{\varphi}=D\int_F \nabla\varphi\, d\underline{F}$$

The flux through the surface of cell i is the sum of fluxes through n_{ij} channels with surface ε each to all N_i neighbouring cells. The channels are assumed to be bidirectional:

$$V\frac{\partial}{\partial t}\bar{\varphi}=D\sum_{\substack{j\\ j\neq i}}^{N_i} n_{ij}\int_{F_\varepsilon}\frac{\partial}{\partial x}\varphi\, d\varepsilon$$

The partial derivative can be calculated with regard to x:

$$V\frac{\partial}{\partial t}\bar{\varphi}_i=D\sum_{\substack{j\\ j\neq i}}^{N_i} n_{ij}\int_{F_\varepsilon}\frac{(\bar{\varphi}(x+\Delta x)-\bar{\varphi}(x))}{\Delta x}d\varepsilon$$

Replacing x by the discrete indices of the adjacent cells gives:

$$V\frac{\partial}{\partial t}\bar{\varphi}_i=D\sum_{\substack{j\\ j\neq i}}^{N_i} n_{ij}\int_{F_\varepsilon}\frac{(\bar{\varphi}_j-\bar{\varphi}_i)}{\Delta x}d\varepsilon=\sum_{\substack{j\\ j\neq i}}^{N_i} n_{ij}\frac{(\bar{\varphi}_j-\bar{\varphi}_i)}{\Delta x}\varepsilon$$

Hence

$$\frac{\partial\bar{\varphi}_i}{\partial t}=\alpha\sum_{\substack{j\\ j\neq i}}^{N_i} n_{ij}(\bar{\varphi}_j-\bar{\varphi}_i) \tag{2}$$

with $\alpha=D\varepsilon$.

We take $n_{ij}\alpha\leq 1/N_i$ as condition for the convergence of the diffusion. For two neighbours one obtains

$$\frac{\partial \bar{\varphi}_i(t)}{\partial t} = \alpha(n_{i,i-1}(\bar{\varphi}_{i-1} - \bar{\varphi}_i) + n_{i,i+1}(\bar{\varphi}_{i+1} - \bar{\varphi}_i)) \tag{3}$$

and if $n_{i,j}=n$ for all cells connected it simplifies to

$$\frac{\partial \bar{\varphi}_i(t)}{\partial t} = \alpha n(\bar{\varphi}_{i-1} + \bar{\varphi}_{i+1} - 2\bar{\varphi}_i) \tag{4}$$

For two neighbours ($N_i=2$) $\alpha n \leq \frac{1}{2}$, hence αn is assumed to be 0.5 for simplicity.

Model parameters

The model parameters are summarized in Table 1. Cell kinetic parameters are known from experiments and are directly transferred into the model (see Potten & Loeffler 1987, Paulus *et al.* 1992). The GF-production rate, the G_1–S threshold parameter, and GF half-life are three linked parameters. They are all hypothetical and reasonable values have to be derived by the simulations. The G_1–S threshold is arbitrarily fixed to be 0.5. The GF production rate and GF half-life determine the profile of the GF concentration. We undertook a systematic screening of the parameter space to find a set of parameters consistent with observed steady state solutions and for post radiation recovery (see below). As a reference set of parameters GF half-life ($t\frac{1}{2}$) was set to 24 h.

The time-increment is an important parameter of any discrete model approach. We conclude from Bjerknes *et al.* (1985) that the diffusion-process takes place on a scale of minutes. Derived from the biological data we assume a time-increment of 0.05 h in our simulations. The assumed cell-loss rate of one cell per cell-column and per hour corresponds to the observed cell migration rate (Cheng & Leblond 1974, Al-Dewachi *et al.* 1979, Kaur & Potten 1986, Loeffler *et al.* 1986, Paulus *et al.* 1993).

Table 1. Model parameters and parameters known by direct observation (Al-Dewachi *et al.* 1979, Tsubouchi & Potten 1985)

	Observation		Model	
	Positions 1–4	Positions 13–16	Positions 1 (relative to Paneth cells)	Position 2 up
Cell cycle				
G_1-phase	4.5 h	3.5 h	>3.5 h	>2.5 h
			≈4.5 h	≈3.5 h
S-phase	8.5 h	7 h	7.5–9.5 h	6–8 h
G_2-phase			1.5 h	0.75 h
M-phase			1.5 h	0.75 h
G_2+M-phase	3 h	1.5	3 h	1.5
T_C: cell cycle	16 h	12.5 h	≈16 h	≈12 h
Growth factor				
GF production	Not available		0.268 h	0.0/h
GF half-time	Not available		24 h	
G_1–S threshold	Not available		0.5	
Time-increment Δt	Not applicable		0.05 h	
Cell loss per cell column	1 cell/h		1 cell/h	

Stochastic elements

Stochastic elements are included in the model. Random elements are used to model the G_1–S transition, the cell loss at the villus tip, and the choice of cells damaged by radiation. The number of Paneth cells is varied in different simulation runs.

Simulation technique

The simulation is programmed in PASCAL by using a special software environment that was developed in our group to simulate dynamic networks. Diffusion is computed by a pseudo-parallel processing of all cells with interim buffers. A complete computation consists of 100 different simulations starting with 50 cells and 1000 h of pre-run simulation. Perturbations and evaluations take place after the pre-run. Label index (LI), mitotic index (MI), percentage labelled mitoses (PLM) are evaluated with regard to time and position. According to the biological technique the LI is defined as the ratio of labelled cells to all cells. The positional LI presented here is evaluated in relation to the cells at a given position. The MI gives the ratio of mitotic cells to all cells (at a certain cell position). The PLM gives the ratio of labelled mitoses to unlabelled mitoses over time after labelling. A cohort of labelled cells may divide several times. Each time it undergoes mitosis the PLM shows a peak. The distance between peaks provides information about the average cell cycle time. After simulation runs of 100 chains statistical evaluation is performed and a graphic output with the IDL-software package is generated. Error bars of the simulation are calculated as standard errors of the mean. All simulations were computed on HP-UX-715/64 workstations. The typical time spent for one computation was 20 min. A visualization of an animated model-crypt may be found in the WWW using the following URL:
http://www.imise.uni-leipzig.de/~torsten/model.html.

Biological data

The biological data presented in this paper is published elsewhere (Potten 1990, Tsubouchi & Potten 1985). Only a brief summary of the procedures is given here. BDF1 mice, aged 10 and 12 weeks, were housed under conventional conditions. Whole-body γ-radiation was delivered from a 137-caesium source with a dose-rate of 4.5 Gy/min and a total dose of 8 or 12 Gy. At 40 min before sacrifice the animals were injected intraperitoneally with 0.925 MBq of ^{3}HTdR. After histological preparation the positions of tritiated thymidine nuclei were recorded by using the method of autoradiography. Mitoses were scored by position as well. The data presented represent the pooled data of at least four animals with a total of 200 sections for each frequency plot.

RESULTS

Steady-state

Figure 2 shows model simulations for the steady state in the small intestine of mice compared with experimental data. Figure 2a shows the GF profile from the crypt bottom to the villus. Up to the fourth cell-position there is a steep increase in GF concentration. This is caused by a variation of the Paneth cell number in the different model chains simulated. The horizontal line shows the threshold for the G_1–S transition. Approximately at position 15, the GF concentration falls below the threshold. Beyond this point cell cycle transition and further initiation of cell proliferation is impossible. The PLM simulations (Figure 2b) are consistent with experimental data suggesting a correct choice of the cell cycle times. Positional MI and LI frequencies after 40 min also show a very good fit to the experimental

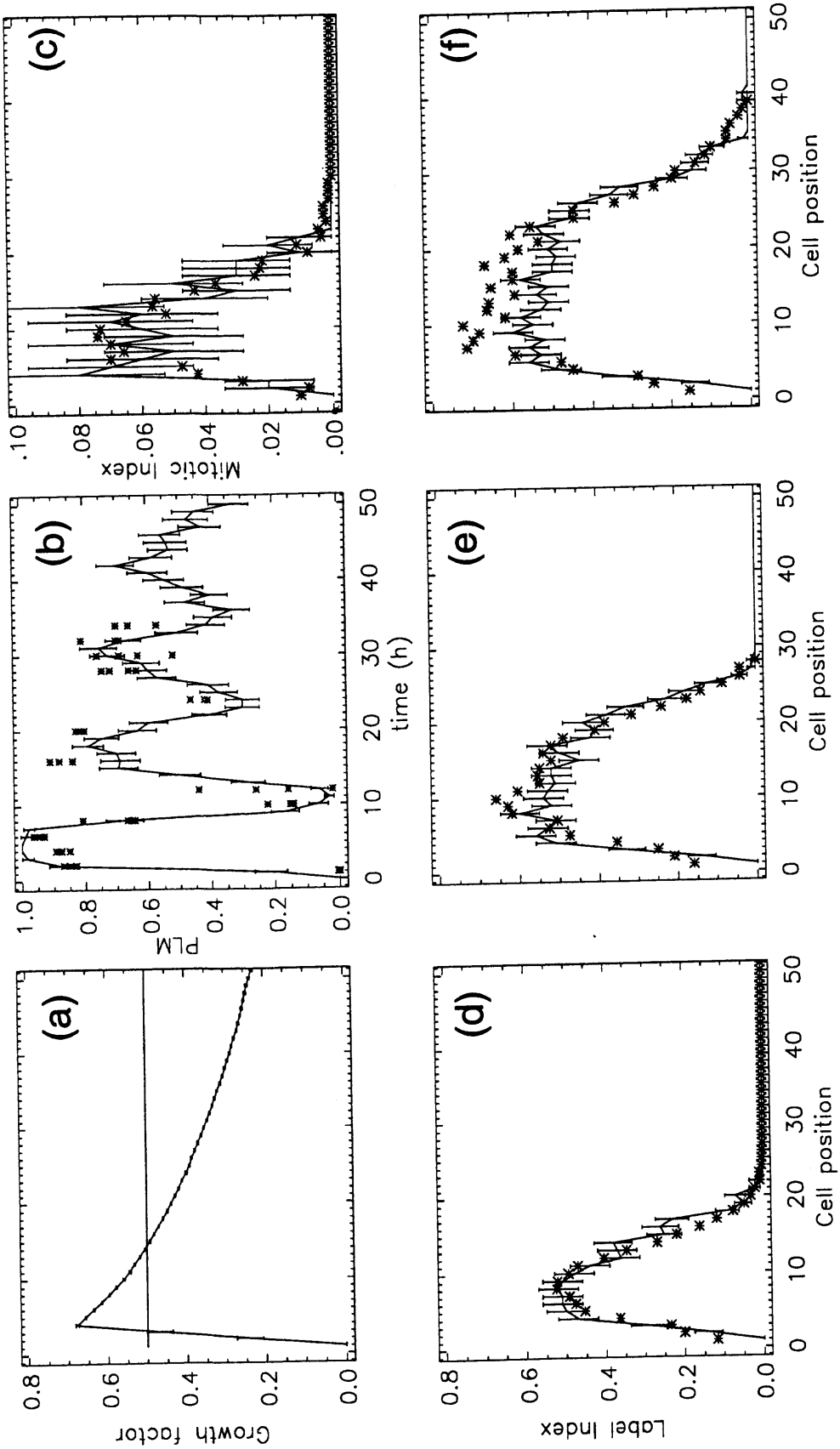

Figure 2. Steady-state: comparison of experimental data with model simulations. (a) Positional growth factor profile in arbitrary units (compare with Figure 1c). (b) Percentage of labelled mitosis (PLM) hours after pulse label (* data, ⌊⌋ simulation). (c) Positional mitotic index (* data, ⌊⌋ simulation). (d) Positional label index 40 min after pulse labelling (* data, ⌊⌋ simulation). (e) Positional label index 6 h after pulse labelling (* data, ⌊⌋ simulation). (f) Positional label index 12 h after pulse labelling (* data, ⌊⌋ simulation).

data (Figures 2c & d). The increase of the curves at the low positions is caused by the non-proliferating Paneth cells. Figures 2e & f show the positional LI frequencies 6 and 12 h after ^{3}HTdR-labelling. Compared to the initial LI (Figure 2d) the leading edge of the distribution is moving to higher positions. This is caused by dividing labelled cells that pass the label to their daughter cells and the cell migration induced by that process. The migration rate of the leading edge is one cell-position per hour. The simulation results fit the experimental data well. Hence this model turns out to generate an adequate description for the steady-state situation.

8 Gy radiation

Figure 3 shows a quantitative comparison of model simulations and experimental data for positional LI frequencies at different times after 8 Gy whole-body irradiation. In the model 60% of all cells lose their proliferation-potential after irradiation and become reproductively sterile. This is followed by a decrease in the cell production causing a decrease of the total cell number as the cell loss at the end of the chain continues at a constant rate. As a consequence the LI drops compared with control (compare Figures 3a & 2d). The recovery starts in the lower crypt beginning from the undamaged proliferative cells. The preceding cell loss leads to a reduced intraepithelial diffusion range and therefore accumulates GF in the lower cells. This causes a prolonged massive stimulation (Figures 3e & f) of cell proliferation, comparable to the observed biological data. The model fits most of the experimental data and the positional LI frequencies. Having fixed all parameters identically for the 8 and 12 Gy radiation data the model does not generate the large overshoot observed at 72 h (Figure 3d). We comment on this discrepancy below.

12 Gy radiation

Furthermore a model simulation of the recovery after a 12 Gy radiation has been undertaken here. Ninety per cent of the cells were considered to be reproductively sterile. All other parameters were kept identical to the previous scenario with 8 Gy radiation. The simulation results compare well with the experimental data (Figure 4). Initially the model starts with fewer proliferative cells than actually observed. Hereafter the overshoot in proliferation can be obtained up to 120 h after radiation (Figure 4f).

Alternative parameters

Variation of the half-time

The choice of the parameters for GF production rate and GF half-life was made after screening the parameter space for optimum results to fit the steady-state and post-radiation scenaria. Figure 5 illustrates the choice. GF half-lives longer than 100 h result in long-term oscillations of the system. At the lower end (below $t\frac{1}{2}$=0.5 h) only very prolonged recoveries after a perturbation occur which are inconsistent with the experimental observations.

The onset of recovery and the timing and magnitude of the overshoot after irradiation turn out to be dependent on the combination of GF half-life and GF production rate. The combination of a short GF half-life and high GF production rate produces a proliferation recovery with an early onset due to the fast supplies of GF but almost no proliferation overshoot in terms of cell numbers due to the fast decay of the accumulated GF (Figures 6a & b). This results in a fast recovery of the cell production rate but a very delayed recovery of the system length.

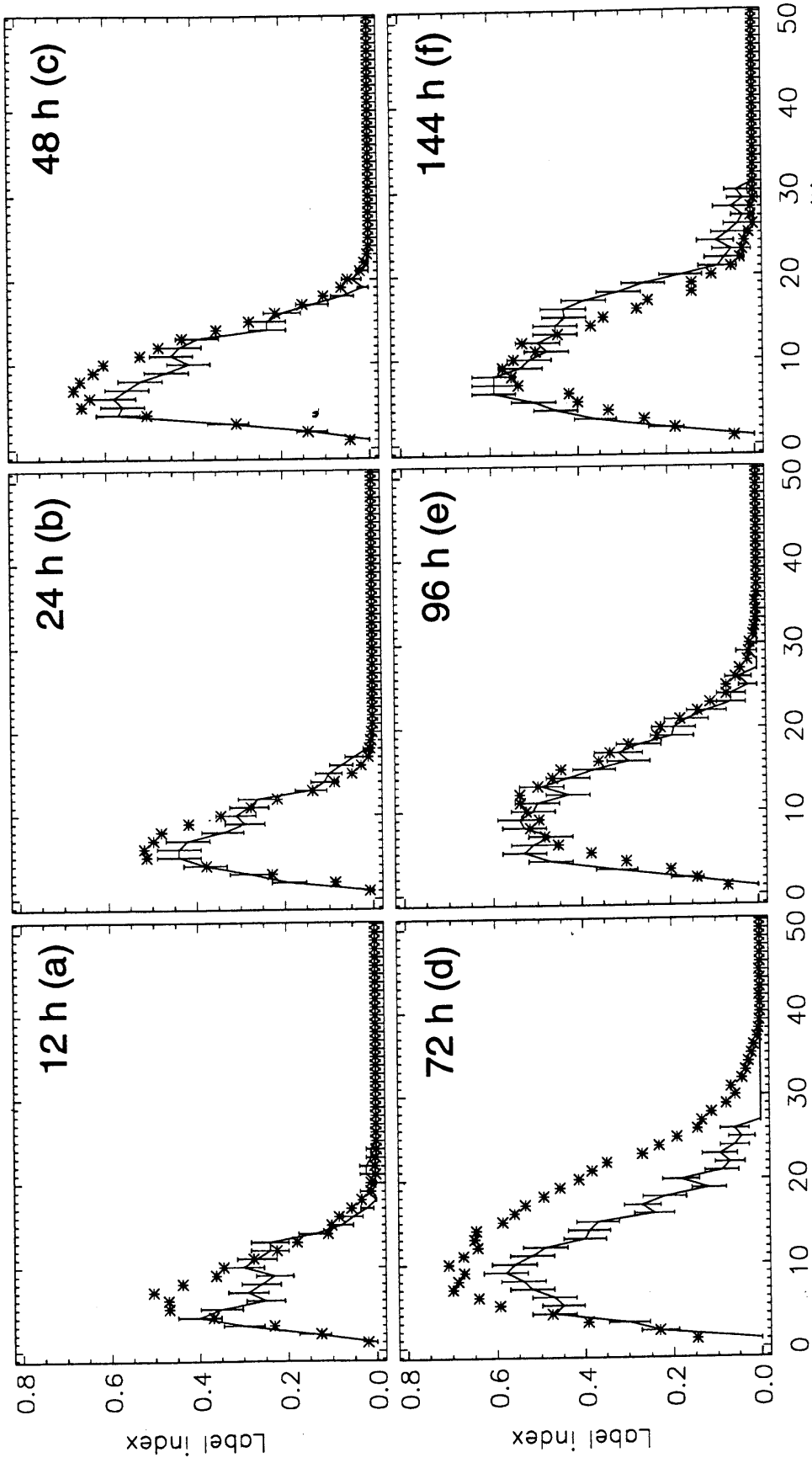

Figure 3. Behaviour after 8 Gy radiation: Comparison of experimental data with model simulations. Positional label index 40 min after pulse labelling. (a) 12 h, (b) 24 h, (c) 48 h, (d) 72 h, (e) 96 h, (f) 144 h after 8 Gy radiation (* data, ⊔ simulation).

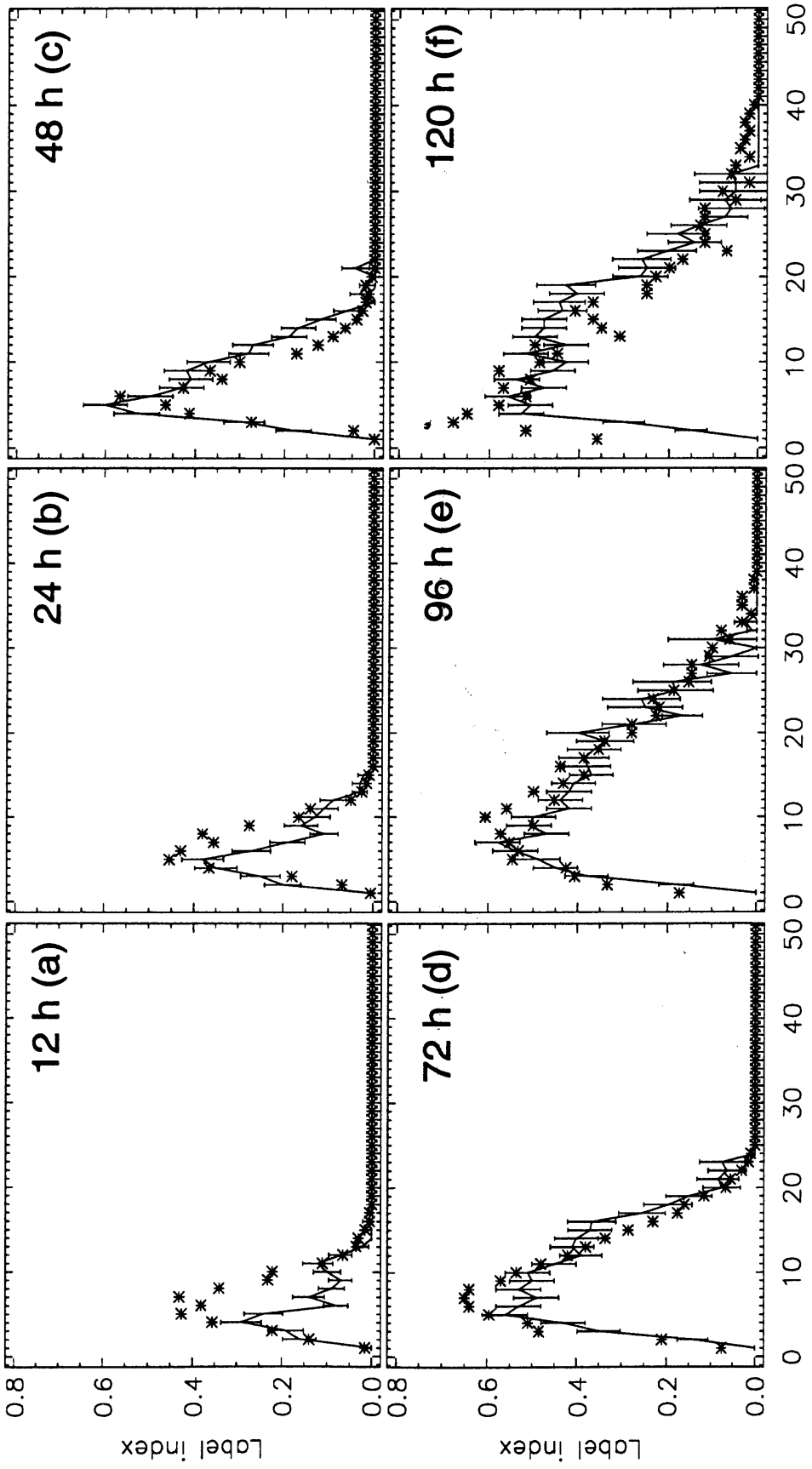

Figure 4. Behaviour after 12 Gy radiation: Comparison of experimental data with model simulations. Positional label index 40 min after pulse labelling. (a) 12 h, (b) 24 h, (c) 48 h, (d) 72 h, (e) 96 h, (f) 120 h after 12 Gy radiation (* data, ⊔ simulation).

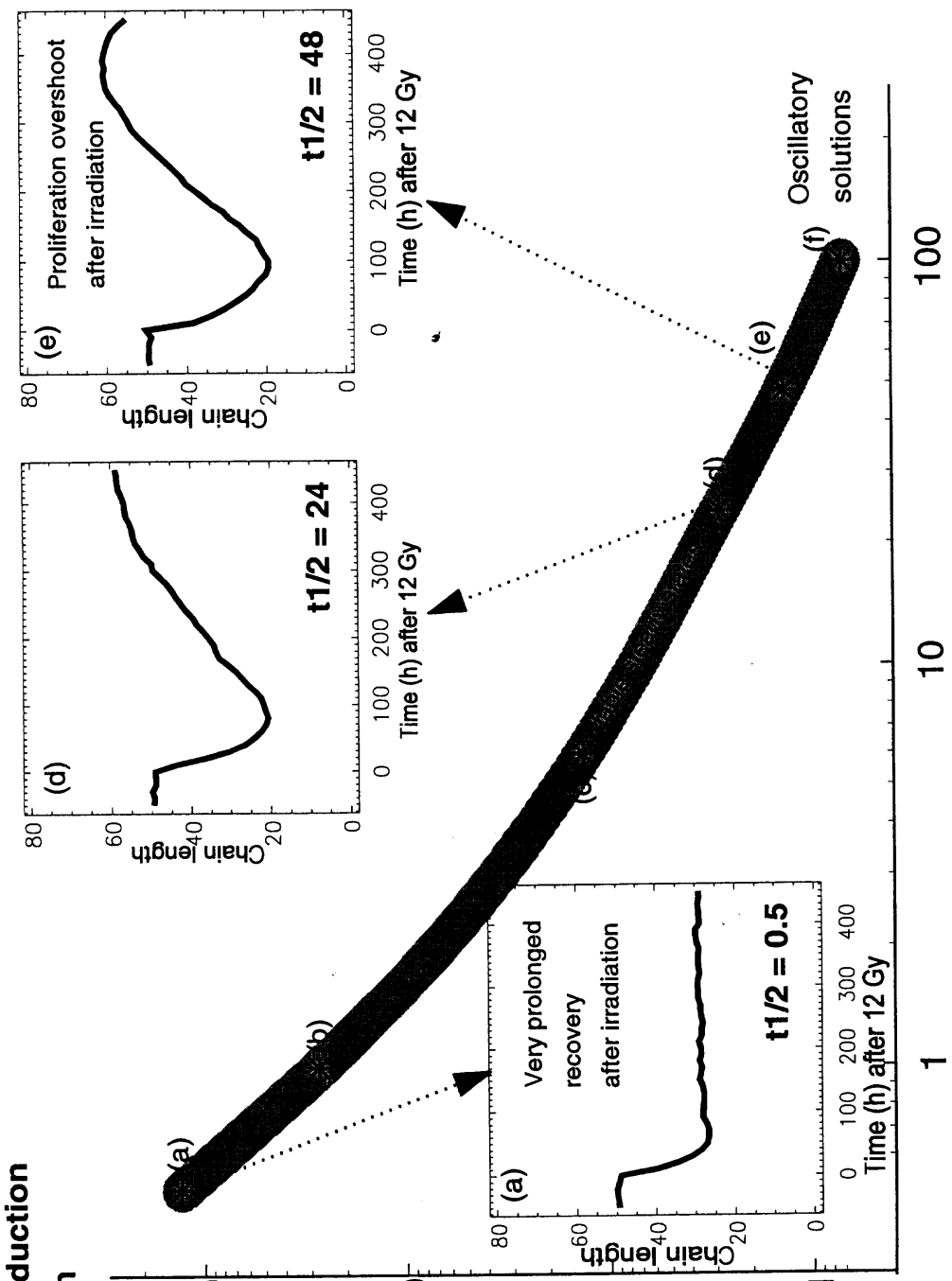

Figure 5. Parameter space for growth factor properties. GF production rate and half-life determine the growth factor profile. Model simulations showed that only parameter constellations within the grey shaded region provide stable steady state solutions (excess proliferation above and lack of proliferation under the curve). Some of them, however, are inconsistent with the data. At the left-hand side (a) recovery after irradiation tends to be far too slow to be consistent with the data. At the right-hand side (f) solutions tend to overshoot too much. Parameter constellations between (c) and (d) seem to be compatible with available data indicating that the half lifetime of the hypothetical growth factor should be within the order of 10–40 h.

The combination of a long GF half-life and a low GF production rate produces an overshoot in proliferation with a late onset due the low GF production but an extended proliferation overshoot due to the slow decay of the accumulated GF (Figures 6c & d). This results in an amplification of the initial damage and a slow recovery of the cell production with an extended late overshoot in cell production and system length.

Radiation induced damage of the cell-to-cell communication

Overshooting proliferation may also be obtained if one assumes perturbations of the gap-junction diffusion process after radiation. In Figure 7 we assume that damaged cells in addition to being reproductively sterilized lose two-thirds of their gap-junctions. This results in long lasting overshoots of proliferation in the recovery phase after radiation. Using this assumption in the simulation of the 9 Gy radiation one obtains an improved fit to the experimental data and the overshoot in proliferation after 48 h (Figure 7, compare Figure 3).

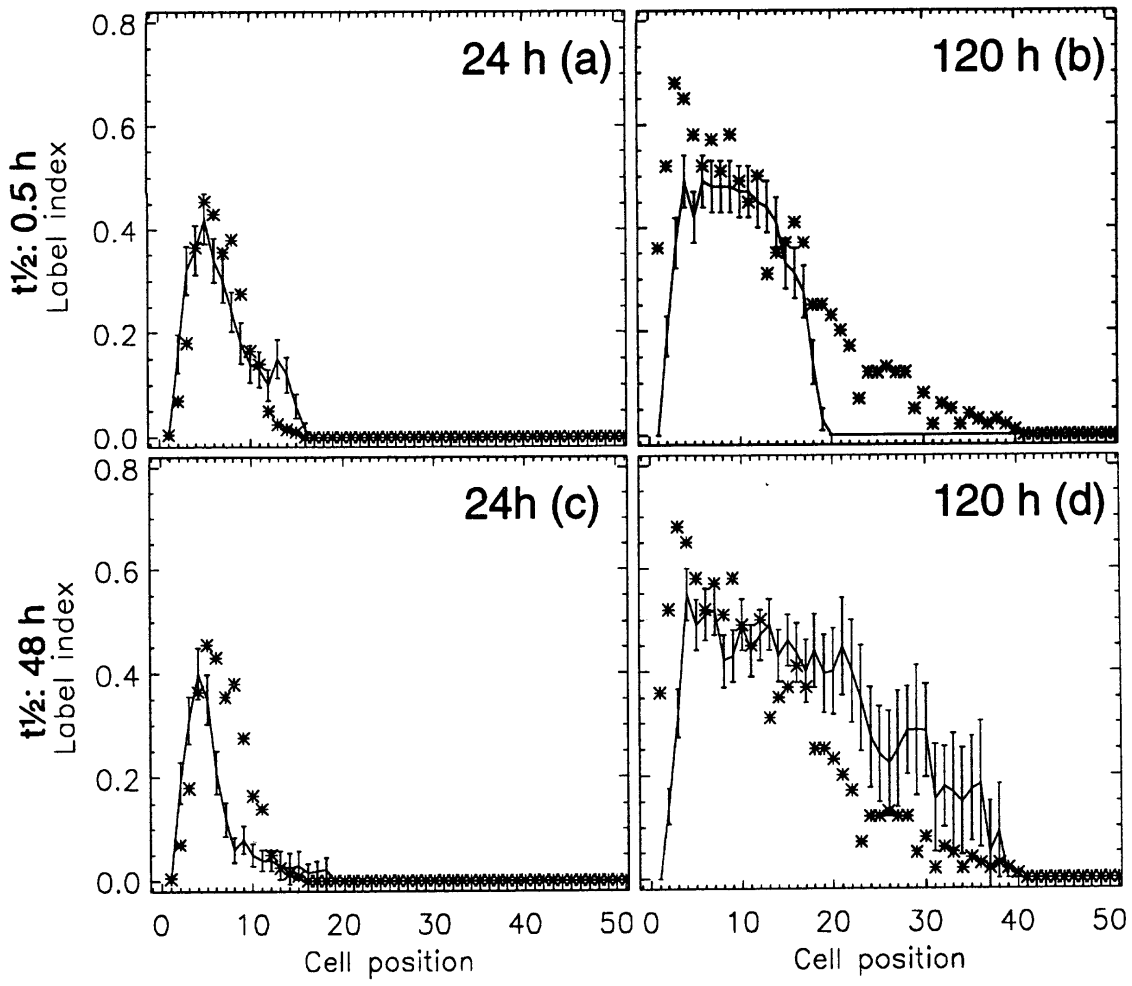

Figure 6. Alternative GF production rate and half-life parameters. Behaviour after 12 Gy radiation. Comparison of experimental data with model simulations. Positional label index 40 min after pulse labelling. (a) Half-life $t_{\frac{1}{2}}$ 0.5 h, 12 h after 12 Gy. (b) Half-life $t_{\frac{1}{2}}$ 0.5 h, 120 h after 12 Gy. (c) Half-life $t_{\frac{1}{2}}$ 48 h, 12 h after 12 Gy. (d) Half-life $t_{\frac{1}{2}}$ 48 h, 120 h after 12 Gy. (* data, ⌊⌋ simulation). Compare with Figure 4; see Figures 5a & e.

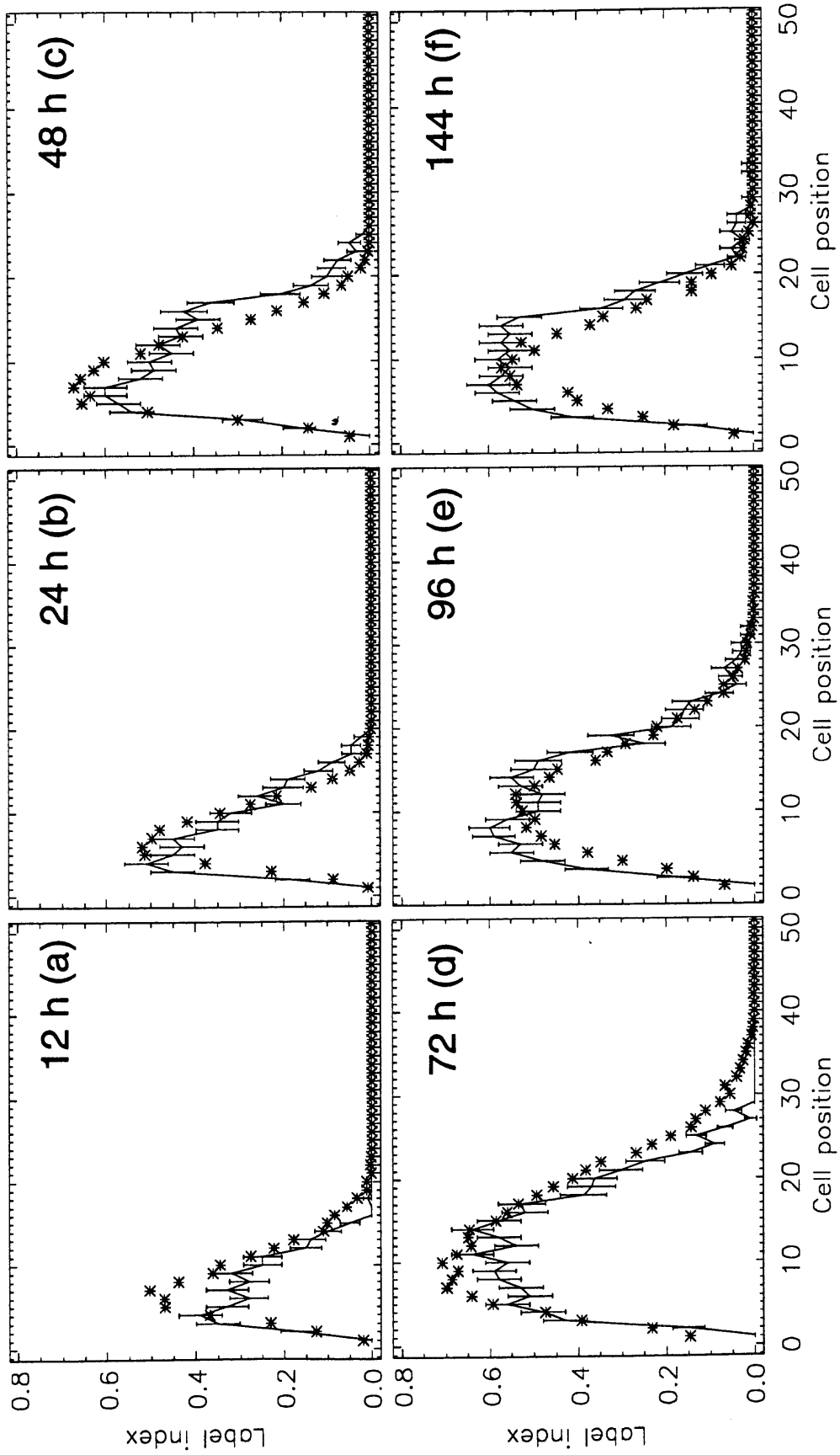

Figure 7. Parameter variation. Behaviour after 8 Gy radiation with perturbed cell-to-cell communication (two-thirds of gap-junction are lost after radiation). Comparison of experimental data with model simulations. Positional label index 40 min after pulse labelling. (a) 12 h, (b) 24 h, (c) 48 h, (d) 72 h, (e) 96 h, (f) 144 h after 8 Gy radiation (* data, ⊔ simulation). Compare with Figure 3.

DISCUSSION AND CONCLUSIONS

The major conclusion drawn from the above model simulations is that an intercellular, intraepithelial growth factor mediated control is sufficient to explain the proliferative behaviour of the intestinal columnar cells in the steady state and following severe perturbations.

In this model all columnar cells in a crypt have the same proliferation potential. Each cell can be triggered to divide if the intraepithelial growth factor exceeds a certain threshold. Hence, this model does not make distinctions between stem cells, transit cells and mature cells. It does not require a pedigree assumption. Furthermore it describes a dynamic feature on how the system reacts after perturbation and how it swings back to a steady state in relation to the spatial arrangement. In this context the model is more powerful than the previous lattice based models whose applicability was restricted to the steady state only.

Limitations of the model

There are a number of limitations inherent in the model.

First, our knowledge of gap-junctional function in proliferation control in the intestinal epithelium is still limited. Therefore the concept of growth factor control mediated by intracellular communications remains somewhat speculative. Gap junctions are only one of a range of possible hypothetical intercellular communication systems. One result of our simulation is that a real transmitter molecule should have a half-life in the order of a day. This is a long time for a growth factor. Only one type of growth factor has been considered. Interactions between stimulatory and inhibitory factors are also possible. The knowledge of the molecules and mechanisms involved in the single decision to enter S-phase is more sophisticated than the simplified model assumption of a single G_1 restriction point.

Second, there are dimensional restrictions. The topology was regarded only in a simple one-dimensional manner. However, a villus is a confluence of approximately 6–10 crypts, each containing approximately 16 cell-columns. Therefore it is difficult to model the crypt-villus transition and the topology of the villus. Efforts are under way to extend the model to a three-dimensional crypt epithelium.

Third, irradiation induced damage was regarded in a simple manner. Acute cell death and short-term G_2-arrests were not considered. Furthermore sterile cells were generally assumed to maintain their gap-junctions at a fixed number disregarding a possible temporal dynamic. Undamaged cells are assumed to proliferate as normal. A cell-cycle arrest of all cells after perturbation was not considered. The growth factor producing cell is assumed not to be perturbed by the irradiation. Due to the dimensional restrictions of the model a loss of this cell would cause a complete standstill in proliferation and the loss of the cell chain. In a two-dimensional crypt model there, however, would be several such sources and an obvious question would be to see how the number can be regulated and can recover after damage.

Stem cells

The concept of stem cells and their regulation has not been the major subject of this work. It is tempting to speculate that the GF producing cells are the stem cells with the properties of proliferation, self-maintenance and the production of many other cells. In fact in our model all columnar cells (even those at the far end of the chain) are potential stem cells and may become clonogenic if the GF concentration exceeds the threshold and they are placed at the crypt bottom. This is contrary to pedigree concepts. On the other hand the GF-producing cell would have a distinct property different from the other columnar cells.

The question of stemness would then fall in two different aspects. The columnar cells at the bottom of a crypt would be those from which all epithelial cell originate as they populate the crypt in the long run. The growth factor producing cells could be different cells, they may even have a turnover, but a specific mechanism must assure that the GF production is localized in the lower part of the crypt. If this localizing mechanism fails and GF production is shifted to another (e.g. higher) position in the crypt unusual proliferative patterns may result.

Villus-crypt feedback

The existence of villus-crypt feedback signals have long been suggested. There are several models based on the assumption of a villus-crypt feedback after radiation (Sato *et al.* 1972, Cairnie 1976, Rijke *et al.* 1976, Britton, Wright & Murray 1982, Yakovlev & Zorin 1988, Meinzer *et al.* 1990). However, the observed regulatory effects could also be explained without any villus-crypt feedback (Paulus *et al.* 1992). The assumption of a regulation restricted to the crypt base, with dynamic regulation of stem and transit-cells was shown to be consistent with many features of post-radiation recovery. The new model proposed here describes a new class of mechanisms not requiring any villus-crypt feedbacks. Furthermore this model is consistent with the fact that the earliest proliferative phases of regeneration in the crypt occur before any change on the villus can be detected (Potten 1990).

Variation of the model

Further simulations showed that a better fit to the experimental data can be achieved if a perturbation of the cell-to-cell communication via gap-junctions is taken into account. After irradiation the partial block of GF diffusion, causes an accumulation of GF in lower columnar cells which leads to a massive stimulation of the proliferation. Consideration of damage and recovery of gap-junctional channels may improve the model fit.

Perspective

The major implication of this work is that intraepithelial growth factors need to be investigated in greater detail. Further biological data on the functionality of the gap-junctions and the GF are needed. The effects of linoleic or retinoic acid on gap-junction permeability *in vitro* (Metha & Loewenstein 1991) may be used to test the model without specific knowledge of the GF.

It is tempting to speculate that the GF production or degradation rate are subject to regulation by systemic hormones or circulating growth stimulatory or inhibitory substance like KGF or TGFβ. In this respect it should be considered that the GF concept we suggest here may provide some kind of a common intraepithelial second messenger mechanism. However, at present no such things are known.

A generalization to a three-dimensional model of the gut epithelium needs to be derived to obtain an acceptable coherence of proliferation and migration along the axis. A three-dimensional approach would enable us also to model the stem-cell regulation. Assuming a short range lateral inhibitory effect of the GF on adjacent GF-producing cells one may obtain a model with only one growth factor that consistently explains stem cell self-organization and proliferation control of the transient cell population.

An application of this approach to other tissues with spatial organization, for example, the colonic crypt but also other epithelia like the skin and oral mucosa may result in interesting new insights into the regulation of proliferation.

In summary we have presented a novel model for proliferation and differentiation control in the intestinal epithelium based on intercellular intraepithelial growth factor diffusion which can simulate biological data in steady-state and after radiation perturbation.

ACKNOWLEDGEMENT

This work has been supported by Deutsche Forschungsgemeinschaft Lo 342/4-2 and the Cancer Research Campaign.

REFERENCES

AL-DEWACHI HS, WRIGHT NA, APPLETON DR, WATSON AJ. (1975) Cell population kinetics in the mouse jejunal crypt. *Virchows Arch. B Cell. Pathol.* **18**, 225.

AL-DEWACHI HS, APPLETON DR, WATSON AJ, WRIGHT NA. (1979) Variation in the cell cycle time in the crypts of Lieberkuhn of the mouse. *Virchows Arch. B Cell. Pathol. Incl. Mol. Pathol.* **31**, 37.

APPLETON DR, AL-DEWACHI HS, MORLEY AR *et al.* (1983) Autoradiographic investigations of cell proliferation in the small and large bowel of the mouse and the jejunal response to some abnormal conditions. *Acta Histochem. Suppl.* **27**, 185.

APPLETON DR. (1990) The use of computer simulation in the design and analysis of cell proliferation experiments. *Acta Histochem. Suppl.* **39**, 131.

ARTIS D, POTTEN CS, ELSE KJ, GRENCIS RK. (in preparation) Immuno-regulation in the murine intestinal epithelium during a mucosal infection: Th1 and Th2 cytokines control stem cell proliferation.

BARNARD JA, WARWICK GJ, GOLD LI. (1993) Localization of transforming growth factor beta isoforms in the normal murine small intestine and colon. *Gastroenterology* **105**, 67.

BJERKNES M, CHENG H, ERLANDSEN S. (1985) Functional gap junction in mouse small intestinal crypts. *The Anatomical Record* **212**, 364.

BOISMENU R, HAVRAN WL. (1994) Modulation of epithelial cell growth by intraepithelial gamma delta T cells. *Science* **266**, 1253.

BRITTON NF, WRIGHT NA, MURRAY JD. (1982) A mathematical model for cell population kinetics in the intestine. *J. Theoretic. Biol.* **98**, 531.

CAIRNIE AB. (1976) Homeostasis in the small intestine. In: Cairnie AB, Lala PK, Osmond DG eds. *Stem-cells of Renewing Cell Populations*. New York: Academic Press, 67.

CHENG H, LEBLOND CP. (1974) Origin, differentiation and renewal of the four main epithelial types in the mouse small intestine. I. Columnar cell. *Am. J. Anat.* **141**, 461.

GOODLAD RA, WILSON TJG, LENTON W, GREGORY H, MCCULLAGH KG, WRIGHT NA. (1987) Proliferative effect of urogastrone-EGF on the intestinal epithelium. *Gut* **28**, 27.

GUSTAFSON-SVARD C, LILJA I, HALLBOOK O, SJODAHL R. (1996) Cyclooxygenase-1 and cyclooxygenase-2 gene expression in human colorectal adenocarcinomas and in azoxymethane induced colonic tumours in rats. *Gut* **38**, 79.

HENDRY JH, ROBERTS SA, POTTEN CS. (1992) The clonogen content of murine intestinal crypts: dependence on radiation dose used in its determination. *Radiat. Res.* **132**, 115.

LOEFFLER M, POTTEN CS. (1997) Stem cells and cellular pedigrees — a conceptual introduction. In: Potten CS, ed. *Stem Cells*. London: Academic Press, 1.

LOEFFLER M, STEIN R, WICHMANN HE, POTTEN CS, KAUR P, CHWALINSKI S. (1986) Intestinal cell proliferation. I. A comprehensive model of steady-state proliferation in the crypt. *Cell. Tissue Kinet.* **19**, 627.

METHA PP, LOEWENSTEIN WR. (1991) Differential regulation of communication by retinoic acid in homologous and heterologous junction between normal and transformed cells. *J. Cell Biol.* **113**, 371.

MEINZER HP, SANDBLAD B. (1986) Evidence for cell generation controlled proliferation in the small intestinal crypt. *Cell Tissue Kinet.* **19**, 581.

MEINZER HP, BAUR HJ, SANDBLAD B, RODRIGUES L. (1990) Mögliche Mechanismen zur Proliferations- und Differentiationskontrolle. In: Giani G, Repges R, eds. *Biometrie und Informatik — neue Wege zur Erkenntnisgewinnung in der Medizin, Medizinische Informatik und Statistik*. Berlin: Springer-Verlag, 71.

KATAOKA K, TABATA J, YAMAMOTO M, TOYOTA T. (1989) The association of gap junctions with large particles in the crypt epithelium of the rat small intestine. *Arch. Histol. Cytol.* **52**, 81.

KAUR P, POTTEN CS. (1986) Circadian variation in migration velocity in small intestinal epithelium. *Cell Tissue Kinet.* **19**, 591.

KWAN WB, SHUI C, NING S, KNOX SJ. (1997) Enhancement of murine intestinal stem cell survival after irradiation by keratinocyte growth factor. *Radiat. Res.* **148**, 248.

OHKUSA T, YAMAMOTO M, KATAOKA K *et al.* (1993) Electron microscopic study of intercellular junctions in human gastric mucosa with special reference to their relationship to gastric ulcer. *Gut* **34**, 86.

PAULUS U, LOEFFLER M, ZEIDLER J, OWEN G, POTTEN CS. (1993) The differentiation and lineage development of globlet cells in the murine small intestinal crypt: experimental and modelling studies. *J. Cell Science* **106**, 473.

PAULUS U, POTTEN CS, LOEFFLER M. (1992) A model of the control of cellular regeneration in the intestinal crypt after perturbation based solely on local stem cell regulation. *Cell Prolif.* **25**, 559.

POTTEN CS, LOEFFLER M. (1987) A comprehensive model of the crypts of the small intestine of the mouse provides insight into the mechanisms of cell migration and the proliferation hierarchy. *J. Theoret. Biol.* **127**, 381.

POTTEN CS. (1990) A comprehensive study of the radiobiological response of the murine (BDF1) small intestine. *Int. J. Radiat. Biol.* **58**, 925.

POTTEN CS, LOEFFLER M. (1990) Stem cells: attributes, cycles, spirals, pitfalls and uncertainties lessons for and from the crypt. *Development* **110**, 1001.

POTTEN Cs, OWEN G, HEWITT D *et al.* (1995) Stimulation and inhibition of proliferation in the small intestinal crypts of the mouse after in vivo administration of growth factors. *Gut* **36**, 864.

POTTEN CS, BOOTH C, PRITCHARD DM. (1997a) The intestinal stem cell: the mucosal governor. *Int. J. Exp. Path.* **78**, 219.

POTTEN CS, BOOTH C, HALEY JD. (1997b) Pretreatment with transforming growth factor beta-3 protects small intestinal cells against radiation damage in vivo. *Br. J. Cancer* **75**, 1454.

RIJKE RP, HANSON WR, PLAISIER HM, OSBORNE JW. (1976) The effect of ischemic villus cell damage on crypt cell proliferation in the small intestine: evidence for a feedback control mechanism. *Gastroenterology* **71**, 786.

SATO F, MURAMATSU S, TSUCHIHASHI S *et al.* (1972) Radiation effects on cell populations in the intestinal epithelium of mice and its theory. *Cell Tissue Kinet.* **5**, 227.

STEEB CB, TRAHAIR JF, READ LC. (1995) Administration of insulin-like growth factor-I (IGF-I) peptides for three days stimulates proliferation of the small intestinal epithelium in rats. *Gut* **37**, 630.

TSUBOUCHI S, POTTEN C. (1985) Recruitment of cells in the small intestine into rapid cell cycle by small doses of external γ or internal β-radiation. *Int. J. Radiat. Biol.* **48**, 361.

YAKOLEV AY, ZORIN AV. (1988) Computer Simulation in Cell Radiobiology. *Lecture Notes in Biomathematics*. Berlin: Springer Verlag, 1.